Inorganic Chemistry

ARTICLE

pubs.acs.org/IC

Synthesis, Characterization, Interaction with DNA, and Cytotoxic Effect in Vitro of New Mono- and Dinuclear Pd(II) and Pt(II) Complexes with Benzo[*d*]thiazol-2-amine As the Primary Ligand

EnJun Gao,* Lei Liu, MingChang Zhu, Yun Huang, Feng Guan, XiaNan Gao, Min Zhang, Lei Wang, WanZhong Zhang, and YaGuang Sun

Department of Coordination Chemistry, Shenyang University of Chemical Technology, Shenyang 110142, China

International Key Laboratory of Shenyang Inorganic Molecule-Based Chemistry, Shenyang 110142, China

ABSTRACT: A series of novel Pd(II) and Pt(II) complexes, $[PdL_2Cl_2]\cdot DMF$ (**1**), $[Pd_2(L\text{-}H)_2(bpy)Cl_2]\cdot(H_2O)_2\cdot DMF$ (**2**), $[Pd_2(L\text{-}H)_2(phen)Cl_2]\cdot 2H_2O$ (**3**), $[PtL_2Cl_2]\cdot H_2O$ (**4**), $[Pt_2(L\text{-}H)_2(bpy)Cl_2]\cdot 2H_2O$ (**5**), and $[Pt_2(L\text{-}H)_2(phen)Cl_2]\cdot H_2O$ (**6**), where bpy = 2,2′-bipyridine, phen = 1,10-phenanthroline, and L = 1,3-benzothiazol-2-amine, have been synthesized and characterized. The competitive binding of the complexes to DNA has been investigated by fluorescence spectroscopy. The values of the apparent DNA binding constant, calculated from fluorescence spectral studies, were 3.8×10^6 (K_{app}(**4**)), 2.9×10^6 (K_{app}(**1**)), 2.4×10^6 (K_{app}(**6**)), 2.0×10^6 (K_{app}(**5**)), 1.2×10^6 (K_{app}(**3**)), and 6.9×10^5 (K_{app}(**2**)). The binding parameters for the fluorescence Scatchard plot were also determined. On the basis of the data obtained, it indicates that the six complexes bind to DNA with different binding affinities in the relative order **4** > **1** > **6** > **5** > **3** > **2**. Viscosity studies carried out on the interaction of complexes with Fish Sperm DNA (FS-DNA) suggested that all complexes bind by intercalation. Gel electrophoresis assay demonstrates that all the complexes can cleave the pBR 322 plasmid DNA and bind to DNA in a similar mode. The cytotoxic activity of the complexes has been also tested against four different cancer cell lines. The results show that all complexes have activity against KB, AGZY-83a, Hep-G2, and HeLa cells. In general, the Pt(II) complexes were found to be more effective than the isostructural Pd(II) complexes. The mononuclear complexes exhibited excellent activity in comparison with the dinuclear complexes in these four cell lines. Moreover, on the KB cell line (the human oral epithelial carcinoma), the observed result seems quite encouraging for the six complexes with IC_{50} values ranging from 1.5 to 8.6 μM. Furthermore, apoptosis assay with hematoxylin−eosin staining shows treatment with the six complexes results in morphological changes of KB cells. The results induce apoptosis in KB cells

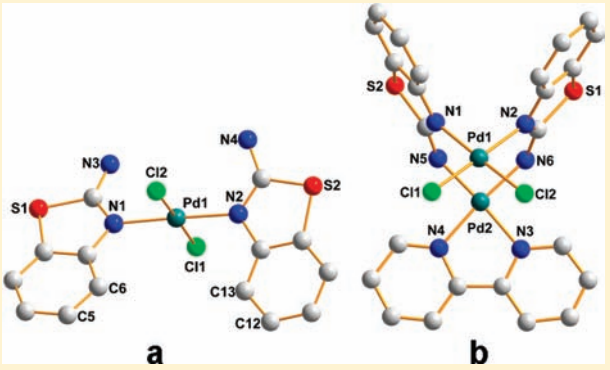

1. INTRODUCTION

Preparation of novel metal complexes has been a main target of medicinal inorganic chemistry because of their potential antitumor activity since the discovery of cisplatin [*cis*-diamminedichloroplatinum(II)] cytotoxic activity.[1] Cisplatin is one of the most effective anticancer drugs in the treatment of a variety of human tumors, and its extensive usage as an antitumor drug has initiated investigations in the medicinal bioinorganic research field toward numerous platinum complexes.[2−4] Unfortunately, its clinical usefulness has frequently been limited by several negative side effects (nephrotoxicity, neurotoxicity, nausea, etc.) and the emergence of cancer cells resistant to cisplatin,[5−7] so it has also stimulated and generated new areas of research, which mainly focused on the search for new metal-based complexes with lower toxicity and more improved therapeutic properties.[8,9]

Many anticancer agents take action through binding to DNA.[10,11] It is believed that the antitumor efficiency of the drug relies on the binding character, binding mode, selectivity toward specific DNA base pairs, and kinetic procedure when it reacts with DNA.[12,13] Nowadays, direct structural analogues of cisplatin have not been found to show improved clinical efficacy compared with the parent drug, most likely because all *cis*-$[PtX_2(amine)_2]$ compounds bind to DNA in a similar DNA binding mode and give rise to a similar biological mode of action. Thus, it is important to look beyond the structure−activity of cisplatin analogues and identify novel materials that can be utilized as potential anticancer agents with activity on cisplatin-resistant model systems, maybe their DNA binding modes quite different from cisplatin.[14,15] Recently, it has been documented that metal-based complexes [where metal = Pd(II), Pt(II)] intercalate between DNA base pairs, building blocks to behave as artificial DNA nucleases generating nicks at different DNA sites.[16−19]

Received: October 24, 2010
Published: April 26, 2011

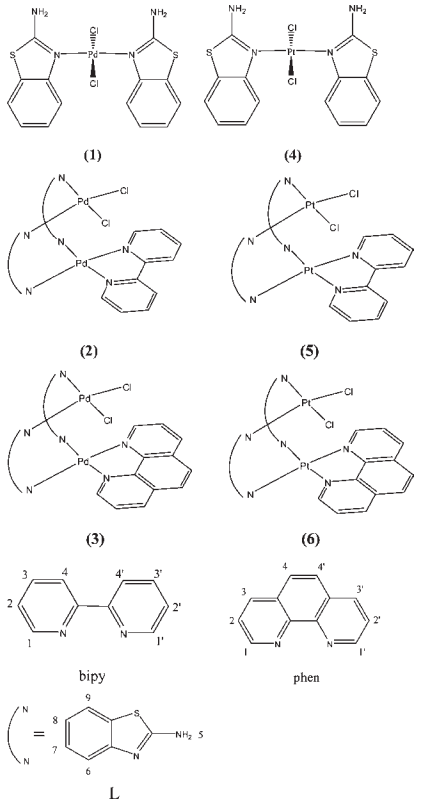

Figure 1. Schematic structure of the six complexes and ligands, and numbering scheme for ^{1}H NMR spectroscopy.

Furthermore, it has been reported that this series of complexes shows significant cytotoxic and antiproliferative effects compared with control.[20]

In a recent paper we reported the synthesis and biological activity of new dinuclear platinum(II) and palladium(II) complexes dibridged by 2,2′-azanediyldibenzoic acid, based on the structural analogy between Pt(II) and Pd(II) complexes.[21] Compared with the number of studies dealing with mononuclear complexes, relatively few studies on dinuclear complexes have been reported to date.[21−26] The interactions between dinuclear complexes and DNA have stimulated us to synthesize new dinuclear copper complexes to evaluate and understand the factors on the DNA binding and cleavage mechanism. One of the best strategies to construct and synthesize dinuclear species is the approach of "complex as a ligand" which contains a potential donor group capable of coordinating to another metal ion.[27] The benzo[*d*]thiazol-2-amine ligand is a favorable ligand to synthesize new dinuclear complexes which contain nitrogen heterocycle, while little research concentrates on the interactions between DNA and complexes bridged by benzo[*d*]thiazol-2- amine.[22,28]

With these facts in mind, we report the synthesis and characterization of mono- and dinuclear complexes with L (L = benzo[*d*]thiazol-2-amine) as a primary ligand (Figure 1). In addition, the interaction of these complexes with fish sperm DNA (FS-DNA) has been examined via fluorescence spectroscopy and viscosity measurements. Their cleavage behavior toward pBR 322 DNA and cytotoxicity in vitro has been also investigated.

2. EXPERIMENTAL SECTION

2.1. Materials and Methods. All chemicals and reagents of reagent grade were commercially available and used without further purification unless otherwise noted. FS-DNA and pBR 322 plasmid DNA were purchased from Sino-American Biotechnology Co. (Beijing, China) and used as received. The KB (human oral epithelial carcinoma) cells, the AGZY-83a (human lung carcinoma) cells, the Hep-G2 (human hepatocellular carcinoma) cells, and the HeLa (human cervix epitheloid carcinoma) cells were obtained from American Type Culture Collection.

Elemental analyses (C, H, N) were carried out on a Perkin-Elmer Series II CHNS/O 2400 elemental analyzer. ^{1}H NMR spectra were measured with a 300 MHz Varian Mercury spectrometer using $CDCl_3$ as solvent. The IR spectra were recorded in a KBr table on a Nicolet IR-470. Fluorescence measurements were performed on a Perkin-Elmer LS55 fluorescence spectrofluorometer.

2.2. Preparation of the Complexes. *2.2.1. Synthesis of [Pd(L)$_2$Cl$_2$]·DMF (**1**).* The complex was prepared as follows. A mixed solution (10 mL) of water and ethanol (1:1) containing 2 mmol (0.3004 g) of L was added dropwise into 10 mL of a water solution containing 1 mmol (0.3264 g) of $K_2[PdCl_4]$ with stirring, and meanwhile, the yellow solid precipitate appeared. The resultant solution was allowed to react for 4 h at room temperature. The yellow deposition was separated from the resultant solution by filtering and redissolved in 10 mL of a mixed solution of DMF and ethanol (1:1), and so the yellow transparent organic mixed solution was obtained and kept in air as well as the filtrate. After a few days, the resulting orange crystals were obtained from the organic mixed solution and then filtered, washed with ethanol, and dried in vacuo. Yield: 42%. Anal. Calcd for $C_{17}H_{19}ON_5S_2Cl_2Pd$ (**1**): C, 37.07; H, 3.48; N, 12.71. Found: C, 37.12; H, 3.52; N, 12.76. IR ν_{max} KBr (cm^{-1}): 3397 ν_{as}(N−H); 3284 ν_s(N−H); 3057 ν(=C−H); 1605 ν(C=N); 1528 ν(C=C); 1446 ν(C=C); 1340 ν(C−N);749 ν-(C−S−C). ^{1}H NMR (DMSO-d_6, 300 MHz; q, quadruplet; t, triplet; d, doublet; s, singlet): δ 7.89 (s, 1H, DMF), 7.66 (d, J = 7.2 Hz, 2H, H6), 7.53 (s, 4H, H5), 7.35 (d, J = 8.1 Hz, 2H, H9), 7.24 (t, J = 9 Hz, 2H, H7), 7.02(t, J = 7.2 Hz, 2H, H8).

*2.2.2. Synthesis of [Pd$_2$ (L-H)$_2$(bpy)Cl$_2$]·2H$_2$O·DMF (**2**).* The complex was prepared as follows. A mixed solution (10 mL) of water and ethanol (1:1) containing 2 mmol (0.3004 g) of L was added dropwise into 10 mL of a water solution containing 2 mmol (0.6528 g) of $K_2[PdCl_4]$ with stirring, and meanwhile, the yellow deposition appeared and the mixture was allowed to react for 4 h at room temperature. Then 10 mL of an ethanol solution of bpy (2,2′-bipyridine) (1 mmol, 0.1562 g) was added, and the deposition became orange. The resultant solution was allowed to react for 2 h at room temperature. The orange deposition was separated from the resultant solution by filtering and redissolved in 10 mL of a mixed solution of DMF and ethanol (1:1), and so the orange transparent organic mixed solution was obtained and kept in air as well as the filtrate. After a few days, the resulting red crystals were obtained from the organic mixed solution and then filtered, washed with ethanol, and dried in vacuo. Yield: 37%. Anal. Calcd for $C_{27}H_{29}O_3N_7S_2Cl_2Pd_2$ (**2**): C, 38.27; H, 3.45; N, 11.57. Found: C, 37.87; H, 3.39; N, 11.25. IR ν_{max} KBr (cm^{-1}): 3359 ν_{as}(N−H); 3261 ν_s(N−H); 3051 ν(=C−H); 1606 ν(C=N); 1540 ν(C=C); 1451 ν(C=C); 1319 ν(C−N); 747ν-(C−S−C). ^{1}H NMR (DMSO-d_6, 300 MHz): δ 8.69 (d, J = 6.3 Hz, 2H, H1, H1′), 8.39(d, J = 8.1 Hz, 2H, H4, H4′), 7.96 (t, J = 7.5 Hz, 2H, H2, H2′), 7.90 (s, 1H, DMF), 7.84(t, J = 7.5 Hz, 2H, H3, H3′), 7.68(d, J = 7.2 Hz, 2H, H6, H6), 7.47(s, 2H, H5, H5), 7.35(d, J = 8.1 Hz, 2H, H9, H9), 7.23(t, J = 6.6 Hz, 2H, H7, H7), 7.04(t, J = 9 Hz, 2H, H8, H8).

*2.2.3. Synthesis of [Pd$_2$(L-H)$_2$(phen)Cl$_2$]·2H$_2$O (**3**).* This complex was synthesized in an identical manner as that described for **2** with phen (1,10-phenanthroline) (1 mmol, 10 mL) in place of bpy. The product was obtained as an orange powder. Yield: 53%. Anal. Calcd for complex

dx.doi.org/10.1021/ic102142j |*Inorg. Chem.* 2011, 50, 4732–4741

Table 1. Crystal Data and Refinement for 1 and 2

	1	2
empirical formula	$C_{17}H_{19}ON_5S_2Cl_2Pd$	$C_{27}H_{29}O_3N_7S_2Cl_2Pd_2$
fw	550.829	847.397
temperature (K)	273(2)	293(2)
wavelength (Å)	0.71073	0.71073
cryst syst	monoclinic	triclinic
space group	*P*2(1)/*c*	*P*-1
a (Å)	12.0721(16)	7.5949(7)
b (Å)	11.4382(15)	12.7708(12)
c (Å)	15.828(2)	17.4310(17)
β (deg)	102.256(2)	81.423(2)
volume (Å^3)	2135.8(5)	1557.6(3)
Z	15	19
D_{calcd} (mg/m^3)	2.530	4.394
absorption coefficient (mm^{-1})	3.957	6.873
F(000)	1515	1919
cryst size	0.355 × 0.110 × 0.042	0.200 × 0.078 × 0.065
θ range for data collection (deg)	1.73−25.71	1.22−26.05
index ranges	$-13 \le h \le 14, -13 \le k \le 11, -19 \le l \le 19$	$-9 \le h \le 9, -15 \le k \le 11, -21 \le l \le 18$
no. reflns collected/unique (R_{int})	11 411/4062(0.0244)	8696/5998(0.0246)
data/restraints/parameters	4062/0/257	5998/0/389
S	1.046	1.050
final *R* indices [$I > 2\sigma(I)$]	R_1 = 0.0448, wR_2 = 0.1234	R_1 = 0.0624, wR_2 = 0.1386
R indices (all data)	R_1 = 0.0553, wR_2 = 0.1326	R_1 = 0.0882, wR_2 = 0.1544
largest diffraction peak and hole (Å e^3)	1.275 and −0.442	1.570 and −1.369

$C_{26}H_{22}N_6O_2S_2C_{l2}Pd_2$ (**3**): C, 39.12; H, 2.78; N, 10.53. Found: C, 38.24; H, 2.80; N, 10.63. IR ν_{max} KBr (cm^{-1}): 3408 ν(O−H); 3367 ν_{as}(N−H); 3256 ν_s(N−H); 3048 ν(=C−H); 1615 ν(C=N); 1540 ν(C=C); 1445 ν(C=C); 1321 ν(C−N); 742 ν(C−S−C). ^{1}H NMR (DMSO-d_6, 300 MHz): δ 9.12 (d, *J* = 6.9 Hz, 2H, H1, H1′), 8.55 (t, *J* = 8.1 Hz, 2H, H3, H3′), 8.03 (s, 2H, H4, H4′), 7.82 (t, *J* = 7.5 Hz, 2H, H2, H2′), 7.65 (d, *J* = 7.8 Hz, 2H, H6, H6), 7.54 (s, 2H, H5, H5), 7.33 (d, *J* = 7.8 Hz, 2H, H9, H9), 7.20 (t, *J* = 7.2 Hz, 2H, H7, H7), 7.00 (t, *J* = 7.2 Hz, 2H, H8, H8).

*2.2.4. Synthesis of the [Pt(L)$_2$Cl$_2$]·H$_2$O (**4**).* This complex was synthesized in an identical manner as that described for **1** with $K_2[PtCl_4]$ (1 mmol, 0.4151 g, 10 mL) in place of $K_2[PdCl_4]$. The product was obtained as a red powder. Yield: 51%. Anal. Calcd for complex $C_{14}H_{14}N_4OS_2Cl_2Pt$ (**4**): C, 28.77; H, 2.41; N, 9.59. Found: C, 28.79; H, 2.46; N, 9.63. IR ν_{max} KBr (cm^{-1}): 3438 ν(O−H); 3395 ν_{as}(N−H); 3290 ν_s(N−H); 3060 ν(=C−H); 1608 ν(C=N); 1527 ν(C=C); 1455 ν(C=C); 1346 ν(C−N); 748 ν(C−S−C). ^{1}H NMR (DMSO-d_6, 300 MHz): δ 7.67(d, *J* = 8.1 Hz, 2H, H6, H6), 7.55(s, 4H, H5, H5, H5, H5), 7.36(d, *J* = 7.2 Hz, 2H, H9, H9), 7.26(t, *J* = 7.2 Hz, 2H, H7, H7), 7.04(t, *J* = 9 Hz, 2H, H8, H8).

*2.2.5. Synthesis of the [Pt$_2$(L-H)$_2$(bpy)Cl$_2$]·2H$_2$O (**5**).* This complex was synthesized in an identical manner as that described for **2** with $K_2[PtCl_4]$ (2 mmol, 0.8302 g, 10 mL) in place of $K_2[PdCl_4]$. The product was obtained as a red powder. Yield: 59%. Anal. Calcd for complex $C_{24}H_{22}N_6O_2S_2Cl_2Pt_2$ (**5**): C, 31.48; H, 1.98; N, 9.18. Found: C, 31.42; H, 2.01; N, 9.13. IR ν_{max} KBr (cm^{-1}): 3419 ν(O−H); 3362 ν_{as}(N−H); 3266 ν_s(N−H); 3082 ν(=C−H); 1611 ν(C=N); 1529 ν(C=C); 1454 ν(C=C); 1326 ν(C−N); 752 ν(C−S−C). ^{1}H NMR (DMSO-d_6, 300 MHz): δ 8.70 (d, *J* = 8.4 Hz, 2H, H1, H1′), 8.40 (d, *J* = 8.1 Hz, 2H, H4, H4′), 7.97 (t, *J* = 7.2 Hz, 2H, H2, H2′), 7.84 (t, *J* = 7.5 Hz, 2H, H3, H3′), 7.68 (d, *J* = 7.2 Hz, 2H, H6, H6), 7.47 (s, 2H, H5, H5), 7.35 (d, *J* = 8.1 Hz, 2H, H9, H9),7.24 (t, *J* = 6.6 Hz, 2H, H7, H7), 7.04 (t, *J* = 9 Hz, 2H, H8, H8).

*2.2.6. Synthesis of the [Pt$_2$(L-H)$_2$(phen)Cl$_2$]·H$_2$O (**6**).* This complex was synthesized in an identical manner as that described for **3** with $K_2[PtCl_4]$ (2 mmol, 0.8302 g, 10 mL) in place of $K_2[PdCl_4]$. The product was obtained as a red powder. Yield: 68%. Anal. Calcd for complex $C_{26}H_{20}N_6OS_2Cl_2Pt_2$ (**6**): C, 30.29; H, 2.33; N, 8.83. Found: C, 30.34; H, 2.27; N, 8.79. IR ν_{max} KBr (cm^{-1}): 3420 ν(O−H); 3352 ν_{as}(N−H); 3253 ν_s(N−H); 3071 ν(=C−H); 1615 ν(C=N); 1540 ν(C=C); 1456 ν(C=C); 1327 ν(C−N); 754 ν(C−S−C). ^{1}H NMR (DMSO-d_6, 300 MHz): δ 9.12 (d, *J* = 7.2 Hz, 2H, H1, H1′), 8.55 (t, *J* = 8.1 Hz, 2H, H3, H3′), 8.03 (s, 2H, H4, H4′), 7.82 (t, *J* = 6.9 Hz, 2H, H2, H2′), 7.65 (d, *J* = 7.5 Hz, 2H, H6, H6), 7.54 (s, 2H, H5, H5), 7.33 (d, *J* = 7.8 Hz, 2H, H9, H9), 7.20 (t, *J* = 7.2 Hz, 2H, H7, H7), 7.00 (t, *J* = 7.2 Hz, 2H, H8, H8).

2.3. X-ray Structure Determination. Single-crystal data of complex **1** and **2** were collected at 293 K on a Bruker Smart 1000 CCD diffractometer with Mo Kα radiation (*k* = 0.71073) in the range of $1.73° < \theta < 25.71°$ and $1.22° < \theta < 26.05°$, respectively. Their structures were solved using direct methods using SHELXL 97[29,30] and refined by full-matrix least-squares methods on F_2. All non-hydrogen atoms were refined anisotropically. Hydrogen atoms were located from different Fourier maps. Structure solution and refinement of complexes **1** and **2** with $I > 2\sigma(I)$ gave R_1 = 0.0448, wR_2 = 0.1236 and R_1 = 0.0588, wR_2 = 0.1352, respectively. Crystal data and structure refinement details are summarized in Table 1.

2.4. Fluorescence Emission Titration. The evidence for complexes **1**−**6** binding to DNA via intercalation is given through the emission quenching experiment. The experiments of DNA competitive binding with ethidium bromide were carried out in the buffer by keeping [DNA]/[EtBr] = 5 ([DNA] = 10 μM, [EtBr] = 2 μM) and varying the concentrations of the metal complexes (0−20 μM). The buffer used in the binding studies was 50 mM Tris-HCl, pH 7.4, containing 10 mM NaCl. The sample was incubated 4 h at room temperature (20 °C)

dx.doi.org/10.1021/ic102142j |*Inorg. Chem.* 2011, 50, 4732–4741

before spectral measurements. For all fluorescence measurements, the entrance and exit slits were maintained at 10 and 10 nm, respectively. The excitation wavelength was 526 nm, and the emission range was set between 550 and 750 nm.

The fluorescence Scatchard plot was performed to study the binding constant determination by the luminescence titration method. Fixed amounts of DNA complex were titrated with increasing amounts of EtBr over a range of EtBr concentrations from 0.5 to 5 μM. An excitation wavelength of 526 nm was used, and the total fluorescence emission intensity was monitored at 605 nm. The experiments were conducted at 20 °C in a buffer containing 5 mM Tris-HCl (pH 7.1) and 50 mM NaCl. Binding data were cast into the form of a Scathchard plot.[31] The concentration of the bound compound was calculated using the equation[32]

$$r_E/C = K(n - r_E)$$

where C is the concentration of free ethidium, r is the ratio of bound complex to total nucleotide concentration [DNA], and n is the maximum value of r_E. The concentration of the free ethidium was calculated using the equation[33]

$$C = [(F_{max} - F)/(F_{max} - F_0)]C_{total}$$

where C_{total} is the total ethidium bromide concentration, F is the observed fluorescence emission intensity at a given EtBr concentration, F_{max} is the intensity in the absence of complex, and F_0 is the fluorescence of the totally bound complex. The plot of r_E/C versus r_E gives the association constant (slope) and the constant binding site size (x intercept) for the agents.

2.5. Viscosity Measurements. Viscosity measurements were carried out using an Ubbelohde viscometer maintained at a constant temperature of 30.0 ± 0.1 °C in a thermostatic bath. FS-DNA samples were prepared by sonication in order to minimize complexities arising from DNA flexibility.[34] Flow time was measured with a digital stopwatch. Each sample was measured at least three times, and an average flow time was calculated. Viscosity values were calculated from the observed flow time of DNA-containing solutions (t) corrected for the flow time of buffer alone (t_0), $\eta = t - t_0$. Data were presented as $(\eta/\eta_0)^{1/3}$ vs binding ratio ([M]/[DNA]),[35] where η is the viscosity value for DNA in the presence of the Pt/Pd (II) complexes and η_0 is the viscosity value of DNA alone.

2.6. Nuclease Activity of the Complexes. The cleavage experiment was carried out in a mixed solution containing Tris buffer (50 mM Tris-acetate, 18 mM NaCl buffer, pH 7.2), pBR322 plasmid DNA (0.33 μg/μL), and different amounts of the complexes, and the mixtures were incubated for 1 h at room temperature. A dye solution (bromophenol blue 0.05%, glycerol 5%, and H_4edta 2 mM) was added to the reaction mixture prior to electrophoresis. The samples were analyzed by electrophoresis at room temperature in the dark for 3 h at 90 V on 0.8% agarose gels in TAE buffer (40 mM Tris-acetate and 2 mM H_4edta, pH 8.0). Then the gel was stained with 1 μg/mL EB (ethidium bromide) and photographed under UV light.

2.7. Cytotoxicity Assay. The in vitro cytotoxicity of complexes **1**−**6** was investigated by the microculture tetrazolium [3-(4,5-dimethylthiazol-2-yl)-2,5-diphenyltetrazolium bromide, MTT] assay[36] on the KB cells, the AGZY-83a cells, the Hep-G2 cells, and the HeLa cells, which were grown in 25 cm^2 tissue culture flasks in an incubator at 37 °C in a humidified atmosphere consisting of 5% CO_2 and 95% air and maintained in logarithmic growth phase in complete medium including RPMI 1640, 10% (v/v) heat-inactivated fetal calf serum, 20 mM Hepes, 0.112% bicarbonate, and 2 mM glutamine. The suspensions of cancer cells were adjusted to cell densities of 5 × 10^5 cells/mL in order to ensure exponential growth throughout drug exposure. Aliquots of 100 μL well of these suspensions were reattributed into 96-well culture plates and preincubated for 24 h. Then cells were exposed to the tested

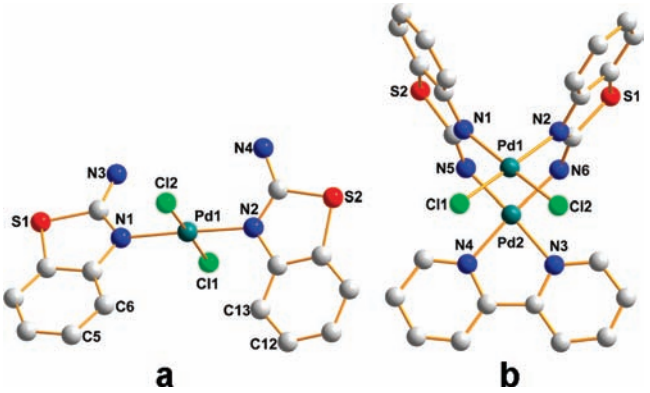

Figure 2. Molecular structures of **1** (a) and **2** (b) showing the local geometry around the metal center and ligands. Thermal ellipsoids were drawn at the 30% probability level (H atoms and solvent molecules were omitted for clarity).

Table 2. Selected Bond Lengths (Angstroms) and Angels (degrees) for 1 and 2

		1	
Pd1−N1	2.021(3)	Pd1−Cl2	2.3135(12)
Pd1−N3	2.025(4)	Pd1−Cl1	2.3234(12)
N1−Pd1−N3	177.42(15)	N1−Pd1−Cl1	90.82(11)
N1−Pd1−Cl2	89.31(11)	N3−Pd1−Cl1	90.48(11)
N3−Pd1−Cl2	89.33(11)	Cl2−Pd1−Cl1	178.31(5)
		2	
Pd1−N2	2.042(6)	Pd2−N5	1.984(7)
Pd1−N1	2.061(6)	Pd2−N6	1.988(8)
Pd1−Cl1	2.432(9)	Pd2−N4	2.009(7)
Pd1−Cl2	2.486(9)	Pd2−N3	2.026(7)
N2−Pd1−N1	88.9(2)	N5−Pd2−N6	89.5(3)
N2−Pd1−Cl1	178.2(2)	N5−Pd2−N4	96.2(3)
N1−Pd1−Cl1	90.8(2)	N6−Pd2−N4	174.3(3)
N2−Pd1−Cl2	88.9(2)	N5−Pd2−N3	175.7(3)
N1−Pd1−Cl2	177.7(2)	N6−Pd2−N3	94.3(3)
Cl1−Pd1−Cl2	91.42(16)	N4−Pd2−N3	80.0(3)

complexes of serial concentrations. The complexes were dissolved in DMF and diluted with RPMI 1640 or DMEM to the required concentrations prior to use (0.1% DMF final concentration). After incubation lasting 72 h, 20 μL of aqueous MTT solution (5 mg/mL) was added to each well and the cells were incubated continually for another 4 h. The media with MTT were removed, and 100 μL of DMSO was added to each well in order to dissolve formazan crystal at room temperature for 30 min. The absorbance of each cell at 450 nm was determined by analysis with a microplate spectrophotometer. The percentage cell viability was determined by dividing the average absorbance of each column of drug-treated wells by the average absorbance of the control wells. Each experiment was repeated three times, and the discussed IC_{50} values represent an arithmetic mean.

2.8. Apoptosis Assay with Hematoxylin−Eosin (H−E) Staining. Hematoxylin−eosin (H−E) staining was carried out as described previously with some modifications.[37] Briefly, KB cells were first grown to 80% confluence on coverslips followed by incubation with concentrations (50 μM) of complexes **1**−**6** for 24 h. Control (untreated), cisplatin, and complexes **1**−**6** treated cells were gently washed twice with cold PBS (phosphate-buffered saline: 137 mM NaCl,

dx.doi.org/10.1021/ic102142j |*Inorg. Chem.* 2011, 50, 4732–4741

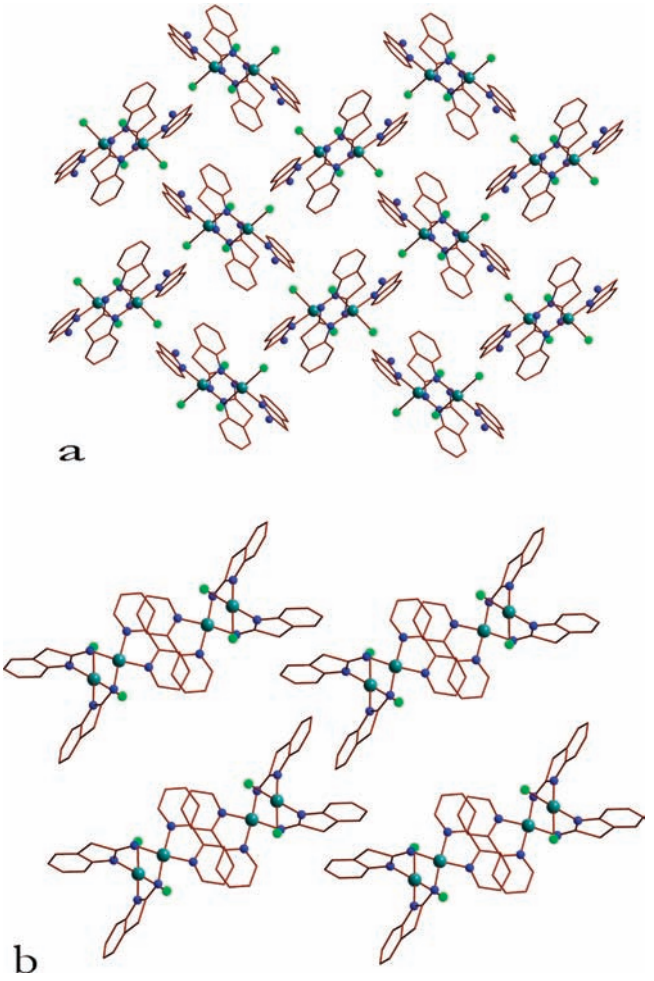

Figure 3. Packing structure of **1** (a) and **2** (b) (H atoms and solvent molecules were omitted for clarity).

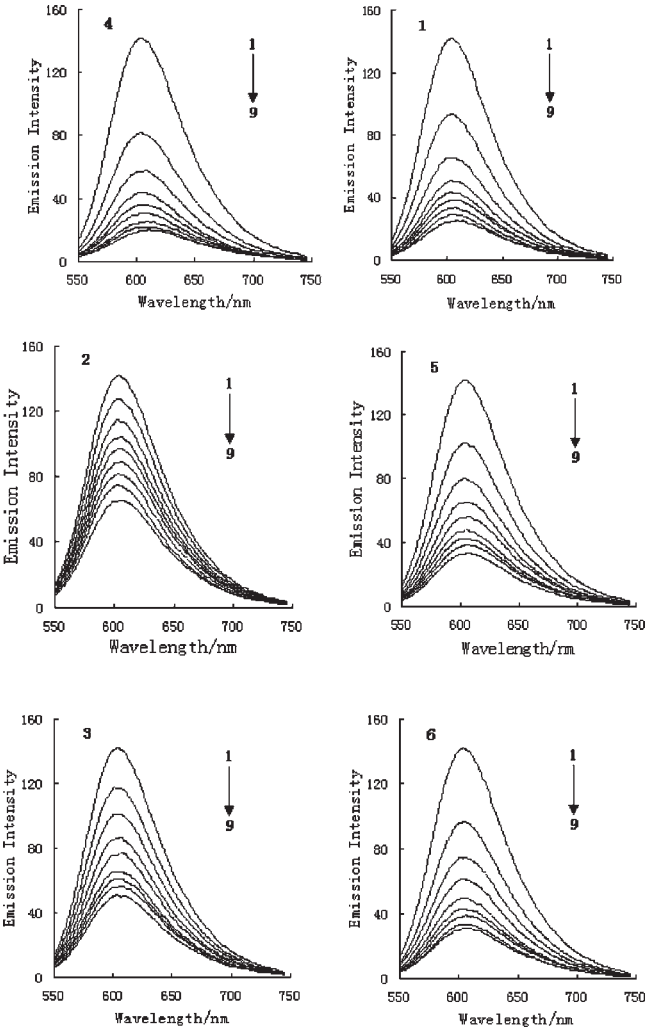

Figure 4. Fluorescence spectra of the binding of EtBr to DNA in the absence (line 1) and presence (lines 2−9) of increasing amounts of the complexes λ_{ex} = 526 nm, C_{EtBr} = 2.0 μM, C_{DNA} = 10.0 μM, $C_{M(1-6)}$ (lines 2−9): 2.5, 5.0, 7.5, 10.0, 12.5, 15.0, 17.5, and 20.0 μM.

2.7 mM KCl, 10 mM Na_2HPO_4, 1.76 mM KH_2PO_4, pH 7.4) and then fixed with 4% paraformaldehyde in PBS for 15 min. Cells were washed three times with PBS, permeabilized with 0.2% Triton X-100 in PBS for 5 min, and washed three times with cold PBS followed by incubation with H-E at 37 °C for 1 h. H−E stained cells were washed three times with cold PBS, mounted on a microscope slide, and visualized under a light microscope fitted with a photometric camera.

3. RESULTS AND DISCUSSION

3.1. Structure of $[Pd(L)_2Cl_2]$·DMF (1) and $[Pd_2(L\text{-}H)_2(bpy)Cl_2]$·2$H_2O$·DMF (2). The crystal structures of complexes **1** and **2** were determined by X-ray crystallography as shown in Figure 2. Selected bond lengths (Angstroms) and angles (degrees) are shown in Table 2.

As can be seen in Figure 2a, complex **1** shows a mononuclear structure and the Pd(II) atom is four coordinated by two chlorine atoms and two nitrogen atoms from the heterocycles of two individual L ligands in the trans configuration. The coordination geometry of the Pd atoms is nearly square planar with rather small deviations of the ligating atoms (the deviated value for the Pd atom is 0.035 Å) from the coordination plane (Cl1/Cl2/N1/N2). The two heterocyclic planes of two individual L molecules form a dihedral angle of 24.79° and are in the same direction in the molecular structure. There is an intermolecular $\pi\cdots\pi$ stacking interaction between two benzene rings from the L ligands, which stabilizes the structure of complex **1** (the shortest distance of centroid-to-centroid between aromatic rings is 3.915 Å). The packing structure of complex **1** is shown in Figure 3a.

The molecular structure of **2** (Figure 2b), determined by X-ray crystallographic methods, consists of a dinuclear Pd_2(II,II) core with a chelating bpy ligand coordinated to one Pd atom, two chlorine atoms coordinated to the other in a syn disposition, and two bridging L occupying the remaining equatorial sites. The coordination geometry of both Pd atoms is nearly square planar with rather small deviations of the ligating atoms (the deviated value for the Pd(1) plane 0.015 and for the Pd(2) plane 0.023) from the coordination plane (Cl1/Cl2/N1/N2 and N3/N4/N5/N6, respectively). The two bridged ligands are stacked in an offset face-to-face mode arrangement like a clamp, conforming to an approximate $\pi\cdots\pi$ interaction. In addition, there is intermolecular $\pi\cdots\pi$ stacking interaction between two benzene rings from individual L ligands and between the pyridine rings from individual bpy ligands (both shortest distances of the centroid-to-centroid between aromatic rings are 3.554 and 3.664 Å, respectively). The Pd···Pd separation distance of

dx.doi.org/10.1021/ic102142j |*Inorg. Chem.* 2011, 50, 4732–4741

2.929 Å is similar to 2.848 Å in the dinuclear palladium complexes $[(bpy)Pd(l\text{-}MeT)_2Pd(bpy)](NO_3)_2 \cdot 5.5H_2O$ (l-MeT = 1-methylthylimine, bpy = 2,2′-bipyridine), which reveal weak metal−metal interactions, but is obviously shorter than those of the reported double-carboxylato-bridged palladium complexes.[21] The stabilization of the metal−metal interaction and bridging the dinuclear structure may be attributed to the strong π-acidic nature of the bpy ligands. Therefore, the different molecular conformation of complexes **1** and **2** may be the origin of their different interactions. The packing structure of complex **2** is shown in Figure 3b.

3.2. Fluorescence Emission Titration. Fluorescence intensities at 605 nm (526 nm excitation) were measured at different complex concentrations. Addition of the complex showed a reduction in the emission intensity. The relative binding propensity of the complexes to FS-DNA was determined from the comparison of the slopes of the lines in the fluorescence intensity versus complex concentration plot.[38] Fluorescence quenching of EtBr−DNA complex can be used to inspect the binding of metal complexes to DNA regardless of their binding modes and only measures their ability to influence the EtBr luminescence intensities in the EtBr−DNA complex.[39] It has previously been reported that the fluorescence intensity of EtBr−DNA could be decreased by addition of the complexes as quenchers, indicating the competition between the complexes and EtBr in binding to DNA.[40,41] It is proof that the complexes intercalate to base pairs of DNA.[42−44] The extent of quenching fluorescence of EtBr−DNA can be used to determine the extent of binding between the complexes and DNA, namely, the binding affinity of the complexes to DNA.

The fluorescence emission spectra of EtBr binding to DNA in the absence and presence of the six complexes are shown in Figure 4. From Figure 4, we can see that an appreciable reduction in the fluorescence intensity is observed on addition of each Pd(II) and Pt(II) complex to DNA pretreated with EtBr, indicating replacement of the EtBr molecules accompanied by intercalation of the complexes.[45,46] From the plot of intensity against complex concentration, the values of the apparent DNA binding constant (K_{app}) were calculated using the equation[47]

$$K_{EtBr}[EtBr] = K_{app}[complex]$$

in which the complex concentration is the value at a 50% reduction of the fluorescence intensity of EtBr and K_{EtBr} = 1.0×10^7 M^{-1} ([EtBr] = 1.3 μM). The K_{app} values are in the series of K_{app}(**4**) (3.8×10^6) > K_{app}(**1**) (2.9×10^6) > K_{app}(**6**) (2.4×10^6) > K_{app}(**5**) (2.0×10^6) > K_{app}(**3**) (1.2×10^6) > K_{app}(**2**) (6.9×10^5). These results suggest that DNA binding with the complexes might be by the intercalation mode.[48] The significantly high K_{app} value for the Pt(II), Pd(II)complexes, in comparison to that of its bpy, phen analogue, could be the result of the presence of its extended aromatic rings which facilitate its DNA binding propensity. The data also indicate that the binding affinity of the mononuclear complexes (**1** and **4**) is larger than that of dinuclear complexes (**2**, **3**, **5**, and **6**), probably owing to the smaller steric hindrance and proper planar structure in the former.[49] Moreover, the result shows that the intercalary ability of the coordinated ligands varies as phen > bpy in this series of complexes.[50]

The fluorescence Scatchard plots obtained for competition of the complex (**1**, **2**, **4**, and **5**) with EtBr to bind with DNA are given in Figure 5. The binding parameters for the fluorescence

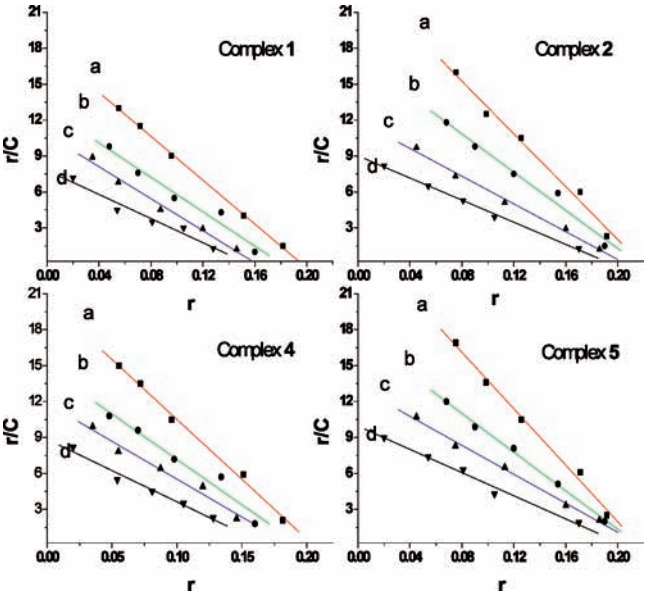

Figure 5. Fluorescence Scatchard plots for the binding of EtBr (0.5−5 M) to DNA in the presence (lines a−d) of increasing concentrations of complexes **1**, **2**, **4**, and **5**.

Table 3. Binding Parameters for the Fluorescence Scatchard Plot of FS-DNA with EtBr in the Presence of Complexes 1, 2, 4, and 5 in Buffer at 20 °C[a]

complex	r_f	K_{obs} ($\times 10^5$ M^{-1})	n
1	0.051 ± 0.005	11.0	0.196 ± 0.001
	0.104 ± 0.010	7.9	0.180 ± 0.002
	1.050 ± 0.010	6.6	0.161 ± 0.003
	2.200 ± 0.020	5.0	0.155 ± 0.004
2	0.051 ± 0.005	9.1	0.218 ± 0.003
	0.109 ± 0.012	7.2	0.215 ± 0.002
	1.030 ± 0.010	6.0	0.206 ± 0.002
	2.060 ± 0.015	4.6	0.195 ± 0.003
4	0.051 ± 0.005	11.7	0.205 ± 0.003
	0.102 ± 0.010	8.1	0.195 ± 0.002
	1.050 ± 0.015	6.3	0.188 ± 0.002
	2.150 ± 0.010	5.2	0.170 ± 0.003
5	0.051 ± 0.005	10.0	0.217 ± 0.002
	0.090 ± 0.015	7.6	0.217 ± 0.002
	1.150 ± 0.020	6.1	0.218 ± 0.003
	2.100 ± 0.025	4.8	0.205 ± 0.003

[a] r_f is the formal ratio of complex to nucleotide concentration with values ranging from 0.51 to 2.2.

Scatchard plot of FS-DNA with EtBr in the presence of complexes are shown in Table 3. Obviously, the plot displays different affinity and binding site size. As shown in Figure 5, both complexes **2** and **5** produce a Scatchard plot in which the slope decreases in the presence of increasing amounts of complex, with little change in the intercept on the abscissa ($0.1951 < x_2 < 0.2183$, $0.2053 < x_5 < 0.2179$). They exhibit a type A behavior. (Type A behavior, competitive inhibition of ethidium binding, produces a Scatchard plot in which the slope decreases in the presence of increasing amounts of metal complex, with no change in the intercept on the abscissa (n).)[51,52] For complexes

dx.doi.org/10.1021/ic102142j |Inorg. Chem. 2011, 50, 4732–4741

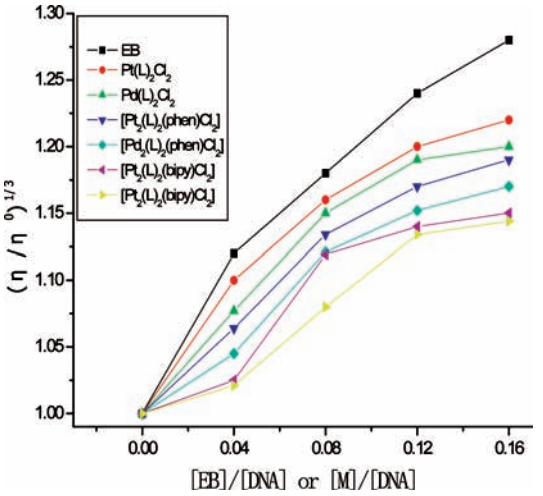

Figure 6. Relative viscosity of FS-DNA (0.50 mM) upon addition of EB, Pt(II), and Pd(II) (0.00−80.00 μM) at 30 ± 0.1 °C, shown as a function of the concentration ratios of [M]/[DNA]: (■) EB, (●) $[Pt(L)_2Cl_2]$ (**4**), (▲) $[Pd(L)_2Cl_2]$ (**1**), (▼) $[Pt_2(L)_2(phen)Cl_2]$ (**6**), (♦) $[Pd_2L_2(phen)Cl_2]$ (**5**), (left pointing solid triangle) $[Pt_2L_2(bpy)Cl_2]$ (**3**), and (right pointing solid triangle) for $[Pd_2L_2(bpy)Cl_2]$ (**2**)). η is the viscosity of DNA in the presence of complex, and η_0 is the viscosity of DNA alone.

2 and **5**, the coordinated geometries around the metal atom are quite similar for the previously reported dinuclear complexes for $[Pd_2(L')_2(bpy)_2]$ and $[Pt_2(L')_2(bpy)_2]$ (bpy = 2,2′-bipyridine and L′ = 2,2′-azanediyldibenzoic dianion).[21] The data presented in Table 3 illustrate analogous results for the interactions of $[Pd_2(L\text{-}H)_2(bpy)Cl_2]$ (complex **2**) and $[Pd_2L'_2(bpy)_2]$ with DNA. By contrast, complexes **1** and **4** show similar type B behavior with both the slope and the intercept changing (see Figure 5), which do not bind to DNA by a single intercalative mechanism.[52] The type B complexes exhibit both intercalative and covalent interactions with DNA. (Type B behavior illustrated both the slope and the intercept changed with complexes exhibiting both intercalative and covalent interactions with DNA.)[52] These complexes contain a relatively good leaving group (chloride) in the buffers employed. The chloride can be hydrolyzed, forming a positively charged species that can assist the electrostatic interaction of the metal complexes with the DNA strand, followed by intercalation of the planar ligand between the base pairs. Therefore, the combined effect of intercalation and coordination is probable for both $Pt(L)_2Cl_2$ and $Pd(L)_2Cl_2$ to allow an effective DNA interaction and cause oxidative damage.[53]

For complexes showing type A or type B behavior, it is possible to evaluate the observed association DNA binding constants. The results listed in Table 3 suggest that mononuclear metal intercalator owns more binding strengths with larger K_{obs}. The present results support this interpretation that intercalation can facilitate the covalent binding of the appropriate metal complexes to DNA.[52]

3.3. Viscosity Measurements. Optical photophysical probes provide necessary but not sufficient clues to support a binding mode, and the viscosity experiment is considered as one of the least ambiguous and most critical tests of the binding modes of complexes to DNA.[54] Therefore, viscosity experiments were performed to investigate the binding mode of these complexes

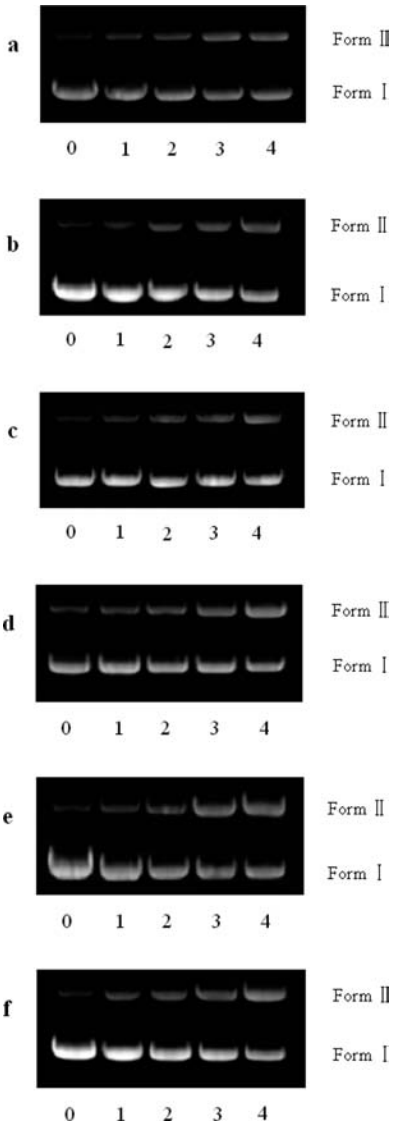

Figure 7. Cleavage of pBR 322 DNA (10 μM) in the absence (lane 0) and presence of complexes (lanes 1−4) at several reactive concentrations: lane 1, 3.3 μM; lane 2, 6.6 μM; lane 3, 13.2 μM; lane 4, 26.4 μM: (a) complex **1**; (b) complex **2**; (c) complex **3**; (d) complex **4**; (e) complex **5**; (f) complex **6**.

to DNA. Intercalation is expected to increase the DNA viscosity; in contrast, a partial, nonclassical intercalation of the ligand can reduce its viscosity by bending the DNA helix.[55,56] The viscosity of FS-DNA is found to be increased in the presence of **1**−**6**, and the extent of the viscosity increase caused by them is comparable, which is lower than that observed for EtBr measured under the same conditions (Figure 6). As shown in Figure 6, the specific viscosity of the DNA sample increased obviously with addition of the complexes, which provided further support that the binding modes of the Pt/Pd(II) complexes were intercalative in the interactions with FS-DNA.

3.4. Nuclease Activity of the Complexes. Reportedly, the half-life of the DNA phosphate−diester bond is approximately 130 000 years via spontaneous hydrolysis under physiological conditions,[57] and so DNA is naturally stable. Oxidative cleavage of DNA induced by a complex mostly takes place in the presence of UV light, a reducing agent, or H_2O_2 as an additive.[58,59]

dx.doi.org/10.1021/ic102142j |*Inorg. Chem.* 2011, 50, 4732–4741

Table 4. Cleavage (C) of pBR322 by Complexes 1−6 in the Different Concentrations

	percentage of cleavage (C) (%)				
complexes	control	3.3 μM	6.6 μM	13.2 μM	26.4 μM
1	3.1	13.9	22.0	30.6	39.68
2	3.7	6.0	15.3	24.4	35.72
3	3.5	10.3	19.9	21.5	33.46
4	4.0	16.2	24.9	34.1	52.29
5	3.9	12.3	24.7	49.9	50.16
6	3.8	13.0	19.0	28.9	48.08

Table 5. Cytotoxicity of the Complexes against Selected Human Tumor Cells

	in vitro activity ($IC_{50} \pm$ SD, μM)			
complexes	KB	AGZY-83a	Hep-G2	HeLa
1	2.8 ± 0.3	21.4 ± 5.1	18.9 ± 6.5	3.5 ± 0.5
2	8.6 ± 1.6	46.6 ± 13.1	36.4 ± 12.4	10.8 ± 2.1
3	6.8 ± 1.3	40.6 ± 10.9	33.9 ± 9.6	8.3 ± 1.7
4	1.5 ± 0.4	11.9 ± 3.8	10.5 ± 2.5	1.2 ± 0.3
5	4.4 ± 0.7	33.0 ± 7.6	25.3 ± 8.6	5.1 ± 1.5
6	3.4 ± 0.5	27.5 ± 8.5	23.9 ± 6.9	4.3 ± 1.5
cisplatin	1.4 ± 0.2	2.0 ± 0.5	1.8 ± 0.4	0.6 ± 0.1

However, the products of oxidative cleavage are not readily amendable to further enzymatic manipulations, so that its usefulness in molecular biology has been limited.[60,61] All complexes have been found to cleave pBR322 plasmid DNA in the absence of UV light, a reducing agent, or H_2O_2. The cleaving efficiency of all complexes has been assessed by their ability to convert supercoiled pBR322 DNA from form I to form II (no form III is observed) by agarose gel electrophoresis (Figure 7). As shown in Figure 7, no distinct DNA cleavage is observed for the control in which the complex is absent (lane 0); however, with increasing concentration of the six complexes, the amount of nicked DNA (form II) increases gradually whereas the supercoiled DNA (form I) diminishes (lanes 1−4).

The nuclease activity of these complexes can be estimated with the percentage of cleavage (C), which can be calculated according to the equation[62]

$$C = (DII + 2DIII)/(DI + DII + 2DIII)$$

where DI, DII, and DIII are the IDVs of form I (supercoil form), form II (nicking form), and form III (linear form), respectively. The integrated density values (IDV) were given by FluorChem 5500 software. The cleavage percents are shown in Table 4 and indicate that there is more effective DNA cleavage activity in Pt(II) complexes compared with Pd(II) complexes under comparable experimental conditions, maybe due to the different binding affinity of the complexes to DNA.[63−65] Additionally, the amount of helical unwinding induced by a complex bound to closed circular DNA also provides another measurement of DNA binding in an intercalation mode.[66,67]

3.5. Cytotoxicity in Vitro Study. It is commonly believed that DNA is the main target of many antitumor agents.[62] Many anticancer agents take action through binding to DNA. From the experiment of competitive binding with EtBr and nuclease activity, we know that all six complexes can react with DNA. To determine whether newly synthesized complexes have anticancer activity, we performed cytotoxicity in vitro tests for six complexes against the selected human tumor cell lines (KB, AGZY-83a, Hep-G2, and HeLa cells). In parallel, the influence of a widely used anticancer drug, cisplatin, has been also assayed. The IC_{50} values are listed in Table 5.

As shown in Table 5, the IC_{50} values for all of these complexes ranged from 1.2 to 46.6 μM, indicating that all of these complexes

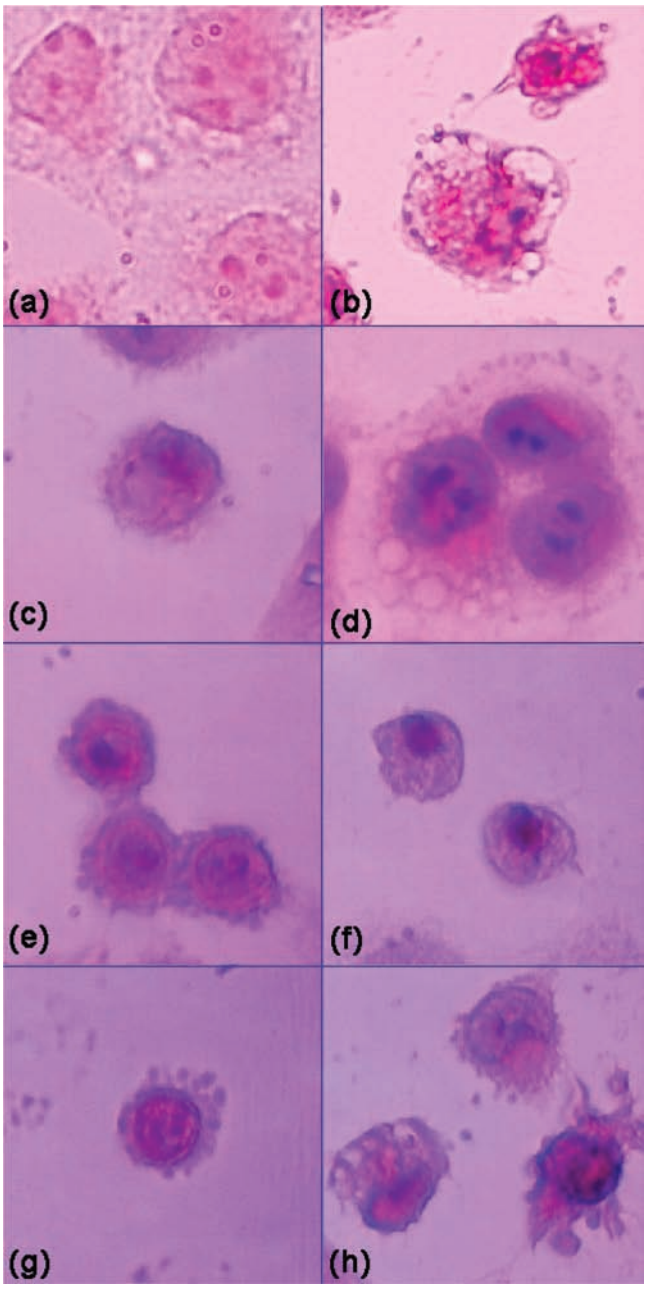

Figure 8. Morphological changes of KB cells. The KB cells were incubated either alone or with complexes for 24 h, stained with H−E, and visualized under light microscope. (a) Untreated control cells. (b) Cells that were treated with 50 μM of cisplatin . (c−h) Formation of apoptotic bodies in cells treated with 50 μM of complexes **1−6**, respectively. Cisplatin was used a positive control.

dx.doi.org/10.1021/ic102142j |*Inorg. Chem.* 2011, 50, 4732–4741

exhibited antitumor activity against all of these cell lines in different degrees. From Table 5, it clearly shows that the complexes are especially effective against KB cell lines and complex **4** showed IC_{50} cytotoxicity coefficients similar to those of cisplatin. It can be seen that complex **4** overcomes the other five complexes to some extent, as is evident from the values in Table 5. Obviously, the dinuclear complexes show lower cytotoxicity in these four cell lines, as in all cases the IC_{50} values are a little higher than the IC_{50} values for mononuclear complexes themselves. Complex **4** $[Pt(L)_2Cl_2]$ is more active toward cell line, and complex **1** $[Pd(L)_2Cl_2]$ takes second place. Both types of complexes show high to modest in vitro cytotoxic properties against various cancer cell lines. The cytotoxic activity induced by complexes **4** and **1** may be explained by the DNA-targeting monofunctional platinum/palladium complexes possessing dual intercalation−coordination property in fact acting as a binder and simultaneously overcoming the cytotoxin. The comparatively low activity of the dinuclear complexes indicates that adduct formed on the DNA helix in the base pairs by dinuclear complex is unable to widen the space to interact on a great effect, probably owing to the some steric hindrance. As a result, the typical 'kink' of cisplatin interaction is not induced. It is therefore evident that the cytotoxicity profile has changed due to the difference between the mono- and the dinuclear coordinated mode.[68]

The mononuclear complexes exhibited excellent activity against the dinuclear complexes listed here. It could be found that the intercalary ability of the coordinated ligands varies as phen > bpy in the same series of complexes. Additionally, the Pt(II) complexes were more efficient than the isostructural Pd(II) complexes, especially against KB cells, showing a high level of resistance against conventional chemotherapeutic agents, because Pd(II) complexes are kinetically more labile and thermodynamically less stable than their analogous Pt(II) complex.[69]

3.6. Apoptotic Study. Apoptosis is a naturally occurring gene-controlled process that plays a critical role in tissue homeostasis and elimination of unwanted cells without affecting normal/unaffected cells.[70] The apoptosis−induction activity on KB cells was observed for **1**−**6** in Figure 8c−h. In Figure 8a, the normal cells exhibited a dense state and an intercellular tight junction, the single cell is polygonal in shape or irregular cell morphology, and cytoplasm has a clear appearance. As expected, in Figure 8b the cells in the positive control (treated with cisplatin at a concentration of 50 μM) were necrotic. Figure 8c−h shows formation of apoptotic bodies in cells treated for 24 h with 50 μM complexes **1**−**6**, where the cell nucleus has become a pyknotic nucleus (shrunken and dark) and condenses chromatin located on the nuclear membrane. The nuclear fragmentation as well as condensation of the nucleus (intense H−E staining) indicated that cells are undergoing apoptotic cell death.[71]

4. CONCLUSIONS

A series of mono- and dinuclear Pt/Pd(II) complexes with benzo[*d*]thiazol-2-amine ligand has been synthesized and characterized in detail by NMR and IR, and two of Pd complexes have been investigated via X-ray crystal analysis. The mononuclear Pd/Pt(II) was coordinated by two chlorines and two nitrogens from benzo[*d*]thiazol-2-amine(L) ligands in the trans configuration, while the other four dinuclear Pd/Pt(II) complexes are in a benzo[*d*]thiazol-2-amine bridging motif. The DNA binding properties of the complexes were examined by fluorescence spectra, which suggest their involvement in intercalative DNA interaction with different binding affinities. From the parameter of the Scatchard plot, complexes **1** and **4** show the behavior not binding to DNA by a single intercalative mechanism, which the observed effect with DNA seems to be the result of two components, one intercalation and one covalent interaction. By contrast, complexes **2** and **5** exhibit competitive inhibition of ethidium binding by a single mechanism. From the viscosity studies, it is observed that the complexes interact with FS-DNA by intercalation. The capability of cleavage of pBR322 DNA by the complexes was investigated using agarose gel electrophoresis, and the results indicate that all complexes exhibit efficient DNA cleavage. The cytotoxic studies show that the complexes exhibit relative cytotoxic activity against different cell lines tested in general and are especially effective against KB cell lines, and complex **4** showed IC_{50} cytotoxicity coefficients similar to those of cisplatin. The comparatively low activity of the dinuclear complexes indicates that adduct formed on the DNA helix in the base pairs by dinuclear complex is unable to widen the space to interact to a great effect, probably owing to the some steric hindrance. In addition, all complexes are under investigation in our laboratories for apoptosis.

At the moment, the major chemical and biological findings of this study have demonstrated that mono- and dinuclear complexes can indeed show activity in human cancer cells in vitro in a reasonable range of concentrations, indicating that these complexes are very promising candidates as antitumor reagents that could contribute to the understanding of cellular uptake of Pt/Pd complexes. Further studies are warranted to assess their pharmacological properties in vivo and elucidate the actual mechanism of their biological activity.

AUTHOR INFORMATION

Corresponding Author

*Phone: +86 24 89385016. Fax: +86 24 89388211. E-mail: ejgao@yahoo.com.cn.

ACKNOWLEDGMENT

We gratefully acknowledge the Natural Science Foundation of China (no. 20971090), the Science and Technology Projects Fund of Shenyang City (no. F10-215-1-00), and the Foundation of Educational Department of Liaoning Province (no. L2010430).

REFERENCES

(1) Rosenberg, B.; Van Camp, L.; Krigas, T. *Nature* **1965**, *205*, 698–699.
(2) Rosenberg, B. In *Metal Ions in Biological Systems*; Sigel, H., Ed.; Marcel Dekker: New York, 1980; Vol. 2, p 127.
(3) Reedijk, J. *Inorg. Chim. Acta* **1992**, *198*, 873–881.
(4) . In *Chemistry and Biochemistry of a Leading Anticancer Drug*; Lippert, B., Ed.; Wiley-VCH: Weinheim, Germany, 1999.
(5) Pasini, A.; Zunino, F. *Angew. Chem., Int. Ed. Engl.* **1987**, *26*, 615–624.
(6) Farrell, N.; Qu, Y.; Hacker, M. P. *J. Med. Chem.* **1990**, *33*, 2179–2184.
(7) Sykes, A. G. *Platinum Met. Rev.* **1988**, *32*, 170–178.
(8) Sherman, S. E.; Lippard, S. J. *Chem. Rev.* **1987**, *87*, 1153–1181.
(9) Gao, E. J.; Wang, L.; Zhu, M. C.; Liu, L.; Zhang, W, Z. *Eur. J. Med. Chem.* **2010**, *45*, 311–316.
(10) Zeglis, B. M.; Pierre, V. C.; Barton, J. K. *Chem. Commun.* **2007**, *44*, 4565–4579.
(11) Erkkila, K. E.; Odom, D. T.; Barton, J. K. *Chem. Rev.* **1999**, *99*, 2777–2795.
(12) Metcalfe, C.; Thomas, J. A. *Chem. Soc. Rev.* **2003**, *32*, 215–224.

(13) Marcon, G.; Carotti, S.; Coronnello, M.; Messori, L.; Mini, E.; Orioli, P.; Mazzei, T.; Cinellu, M. A.; Minghetti, G. *J. Med. Chem.* **2002**, *45*, 1672–1677.
(14) Miernicka, M.; Szulawska, A.; Czyz, M.; Lorenz, I.; Mayer, P.; Karwowski, B.; Budzisz, E. *J. Inorg. Biochem.* **2008**, *102*, 157–165.
(15) Gao, E. J.; Liu, F. C.; Zhu, M. C.; Wang, L.; Huang, Y.; Liu, H. Y.; Ma, S.; Shi, Q. Z.; Wang, N. *Enzyme Inhib. Med. Chem.* **2010**, *25*, 1–8.
(16) Suggs, J. W.; Dube, M. J.; Nichols, M. *J. Chem. Soc., Chem. Commun.* **1993**, *3*, 307–309.
(17) Gao, E. J.; Zhu, M. C.; Liu, L.; Wang, L.; Huang, Y.; Shi, C. Y.; Zhang, W, Z; Sun, Y. G. *Inorg. Chem.* **2010**, *49*, 3261–3270.
(18) Lempers, E. M.; Rarilla, A.; Suh, M.; Kostic, N. M. In *Book of Abstracts Division of Inorganic Chemistry*; Tullius, T. D., Ed.; National Meeting Spring, No. 362: American Chemical Society: Washington, DC, 1991.
(19) Suggs, J. W.; Higgins, J. D.; Wagner, R. W.; Millard, J. T. *Metal−DNA Interactions*; American Chemical Society; Washington, DC, 1989.
(20) Mital, R.; Srivastava, T. S. *J. Inorg. Biochem.* **1990**, *40*, 111–120.
(21) Gao, E. J.; Zhu, M. C.; Yin, H. X.; Liu, L.; Wu, Q.; Sun, Y. G. *J. Inorg. Biochem.* **2008**, *102*, 1958–1964.
(22) Gao, E. J.; Wang, K. H.; Gu, X. F.; Ying, Y.; Sun, Y. G.; Zhang, W. Z.; Yin, H. X.; Wu, Q.; Zhu, M. C.; Yan, X. M. *J. Inorg. Biochem.* **2007**, *101*, 1404–1409.
(23) Wu, J. Z.; Yuan, L.; Wu, J. F. *J. Inorg. Biochem.* **2005**, *99*, 2211–2216.
(24) Li, Y. P.; Wu, Y. B.; Zhao, J.; Yang, P. *J. Inorg. Biochem.* **2007**, *101*, 283–290.
(25) Zhang, Q. Q.; Zhang, F.; Wang, W. G.; Wang, X. L. *J. Inorg. Biochem.* **2006**, *100*, 1344–1352.
(26) Zhang, F.; Zhang, Q. Q.; Wang, W. G.; Wang, X. L. *J. Photochem. Photobiol. A: Chem.* **2006**, *184*, 241–249.
(27) Ruiz, R.; Faus, J.; Lloret, F.; Journaurx, Y. *Coord. Chem. Rev.* **1999**, *193−195*, 1069–1117.
(28) Joyce, L. L.; Batey, R. A. *Org. Lett.* **2009**, *11*, 2792–2795.
(29) Sheldrick, G. M. *SHELXS 97*; University of Göttingen: Göttingen, Germany, 1997.
(30) Sheldrick, G. M. *SHELXS 97*; University of Göttingen: Göttingen, Germany, 1997.
(31) Satyanarayana, S.; Dabrowiak, J. C.; Chaires, J. B. *Biochemistry* **1992**, *31*, 9319–9324.
(32) Lepecq, J. B.; Paoletti, C. *J. Mol. Biol.* **1967**, *27*, 87–106.
(33) Kumar, C. V.; Asuncion, E. H. *J. Am. Chem. Soc.* **1993**, *115*, 8547–8553.
(34) Chaires, J. B.; Dattagupta, N.; Crothers, D. M. *Biochemistry* **1982**, *21*, 3933–3940.
(35) Cohen, G.; Eisenberg, H. *Biopolymers* **1969**, *8*, 45–55.
(36) Alley, M. C.; Scudiero, D. A.; Monks, A.; Hursey, M. L.; Czerwinski, M. J.; Fine, D. L.; Abbott, B. J.; Mayo, J. G.; Shoemaker, R. H.; Boyd, M. R. *Cancer Res.* **1988**, *48*, 589–601.
(37) Fujikawa, D. G.; Shinmei, S. S.; Cai, B. *Neuroscience* **2000**, *8*, 41–53.
(38) Wang, B.; Yang, Z. Y.; Crewdson, P.; Wang, D. Q. *J. Inorg. Biochem.* **2007**, *101*, 1492–1502.
(39) Mei, W. J.; Liu, J.; Chao, H.; Ji, L. N. *Transition Met. Chem.* **2003**, *28*, 852–857.
(40) Lakowicz, J. R.; Weber, G. *Biochemistry* **1973**, *12*, 4161–4170.
(41) Baguley, B. C.; Bret, M. L. *Biochemistry* **1984**, *23*, 937–943.
(42) Bai, G. Y.; Wang, K. Z.; Duan, Z. M.; Gao, L. H. *J. Inorg. Biochem.* **2004**, *98*, 1017–1022.
(43) Tysoe, S. A.; Kopelman, R.; Schelzig, D. *Inorg. Chem.* **1999**, *38*, 5196–5197.
(44) Han, G. Y.; Yang, P. *J. Inorg. Biochem.* **2002**, *91*, 230–236.
(45) Mansuri-Torshizi, H.; Mital, R.; Srivastava, T. S.; Parekh, H.; Chitnis, M. P. *J. Inorg. Biochem.* **1991**, *44*, 239–247.
(46) Gao, E. J.; Zhao, X. M.; Liu, Q. T.; Xiu, R. *Acta Chim. Sin.* **2004**, *62*, 593–597.
(47) Lee, M.; Rhodes, A. L.; Wyatt, M. D.; Forrow, S.; Hartley, J. A. *Biochemistry* **1993**, *15*, 4339.
(48) Rajendiran, V.; Murali, M.; Suresh, E.; Sinha, S.; Somasundaramc, K.; Palaniandavar, M. *Dalton Trans.* **2008**, *1*, 148–163.
(49) Lin, Q. Y.; Lu, X. H.; Chen, J. R.; Li, L. C.; He, X. Q. *Spectrosc. Spectr. Anal.* **2008**, *28*, 1359–1363.
(50) Ghosh, S.; Barve, A. C.; Kumbhar, A. A.; Kumbhar, A. S.; Puranik, V. G.; Datar, P. A.; Sonawane, U. B.; Joshi, R. R. *J. Inorg. Biochem.* **2006**, *100*, 331–343.
(51) Arakawa, H.; Ahmad, R.; Naoui, M.; Tajmir-Riahi, H. A. *J. Biol. Chem.* **2000**, *275*, 10150–10153.
(52) Howe-Grant, M.; Wu, K. C.; Bauer, W. R.; Lippard, S. J. *Biochemistry* **1976**, *15*, 4339–4346.
(53) Richards, A. D.; Rodger, A. *Chem. Soc. Rev.* **2007**, *36*, 471–483.
(54) Zou, X. H.; Ye, B. H.; Li, H.; Zhang, Q. L.; Chao, H.; Liu, J. G.; Ji, L. N.; Li, X. Y. *J. Biol. Inorg. Chem.* **2001**, *6*, 143–150.
(55) Satyanarayana, S.; Dabrowiak, J. C.; Chaires, J. B. *Biochemistry* **1992**, *31*, 9319–9324.
(56) Satyanarayana, S.; Dabrowiak, J. C.; Chaires, J. B. *Biochemistry* **1993**, *32*, 2573–2584.
(57) Radzicka, A.; Wolfenden, R. *Science* **1995**, *267*, 90–93.
(58) Tan, L. F.; Chao, H.; Liu, Y. J.; Li, H.; Sun, B.; Ji, L. N. *Inorg. Chim. Acta* **2005**, *358*, 2191–2198.
(59) Zhang, Q. L.; Liu, J. G.; Chao, H.; Xue, G. Q.; Ji, L. N. *J. Inorg. Biochem.* **2001**, *83*, 49–55.
(60) Screedhara, A.; Frued, J. D.; Cowan, J. A. *J. Am. Chem. Soc.* **2000**, *122*, 8814–8824.
(61) Mancin, F.; Scrimin, P.; Tecilla, P.; Tonellato, U. *Chem. Commun.* **2005**, *20*, 2540–2548.
(62) Gao, F.; Chao, H.; Zhou, F.; Yuan, Y. X.; Peng, B.; Ji, L. N. *J. Inorg. Biochem.* **2006**, *100*, 1487–1494.
(63) Zhang, Q. L.; Liu, J. G.; Liu, J. Z.; Li, H.; Yang, Y.; Xu, H.; Chao, H.; Ji, L. N. *Inorg. Chim. Acta* **2002**, *339*, 34–40.
(64) Gao, E. J.; Liu, C.; Zhu, M. C.; Lin, H. K.; Wu, Q.; Liu, L. *Curr. Med. Chem.* **2009**, *9*, 356–368.
(65) Qian, J.; Gu, W.; Liu, H.; Gao, F. X.; Feng, L.; Yan, S. P.; Liao, D. Z.; Cheng, P. *Dalton Trans.* **2007**, *10*, 1060–1066.
(66) Shi, S.; Liu, J.; Li, J.; Zheng, K. C.; Huang, X. M.; Tan, C. P.; Chen, L. M.; Ji, L. N. *J. Inorg. Biochem.* **2006**, *100*, 385–395.
(67) Liu, J.; Zheng, W. J.; Shi, S.; Tan, C. P.; Chen, J. C.; Zheng, K. C.; Ji, L. N. *J. Inorg. Biochem.* **2008**, *102*, 193–202.
(68) Roy, S.; Maheswari, P. U.; Lutz, M.; Spek, A. L.; Dulk, H. D.; Barends, S.; Wezel, G. P.; Hartl, F.; Reedijk, J. *Dalton Trans.* **2009**, *48*, 10846–10860.
(69) Eryazici, I.; Moorefield, C. N.; Newkome, G. R. *Chem. Rev.* **2008**, *108*, 1834–1895.
(70) Shakya, R.; Peng, F. Y.; Liu, J. G.; Heeg, M. J.; Verani, C. N. *Inorg. Chem.* **2006**, *45*, 6263–6268.
(71) Awasthi, S.; Singhal, S. S.; Chaubey, N. H.; Zimniak, M. P.; Srivastava, S. K.; Singh, S. V.; Awasthi, Y. C. *Int. J. Cancer* **1996**, *68*, 333–339.